Polarization-maintaining fiber-optic-grating vector vibroscope

Tuan Guo,[1,*] Libin Shang,[1] Fu Liu,[1] Chuang Wu,[1,2] Bai-Ou Guan,[1] Hwa-Yaw Tam,[2] and Jacques Albert[3]

[1]*Institute of Photonics Technology, Jinan University, Guangzhou 510632, China*

[2]*Photonics Research Center, Department of Electrical Engineering, The Hong Kong Polytechnic University, Kowloon, Hong Kong SAR, China*

[3]*Department of Electronics, Carleton University, 1125 Colonel By Drive, Ottawa, Ontario K1S 5B6, Canada*

**Corresponding author: tuanguo@jnu.edu.cn*

Received December 18, 2012; revised January 13, 2013; accepted January 14, 2013;
posted January 15, 2013 (Doc. ID 181842); published February 12, 2013

A fiber-optic vector vibroscope based on orthogonal polarization cladding-to-core recoupling is demonstrated. A compact structure in which a short section of polarization-maintained (PM) fiber stub containing a straight fiber Bragg grating (FBG) is spliced to another single-mode fiber. Two well-defined orthogonally polarized cladding modes reflected by the PM-FBG are recoupled at the junction and the coupling intensity shows an extremely high sensitivity to bending in the corresponding orthogonal directions. Both the orientation and amplitude of the vibrations can be determined unambiguously via dual-path power detection of these recoupled orthogonal-polarimetric cladding modes ($LP_{1,12}$ and $LP_{1,13}$). Since spectral information is not required, temperature changes do not affect the sensor response, and power fluctuations can be referenced out by monitoring the power in the core mode ($LP_{0,1}$) resonance.

OCIS codes: 060.2370, 060.3735.

Fiber Bragg gratings (FBGs) written into high birefringence, polarization-maintaining (PM) single-mode fibers have found wide applications in both optical communications and sensing systems. Such birefringent fibers support two distinct polarization eigenmodes with two effective refractive indices. The FBG couples light polarized along the two principal axes at two different Bragg wavelengths, corresponding to slow and fast axes. Since these eigenmodes have orthogonal-polarimetric mode field shapes and effective indices, they react differently to perturbations inside and outside of the fiber (transversal strain [1], local pressure [2], shear strain [3], and transverse acoustic waves [4]). This device has opened up a multitude of opportunities for single-point sensing in hard-to-reach spaces, with very controllable cross-sensitivities, absolute and relative measurements of various parameters and offers improved sensitivity to refractive index variations when tapering the fiber to micro- or nano-diameters.

However, while early research on PM-FBGs was mainly focused on the core modes properties, the cladding modes of such fibers also have unique mode field shapes and polarization-dependent transmission spectra that can be used for sensing [5,6]. In fact, the polarization dependency of cladding modes has important consequences for sensing even in non-PM fibers. In a prior implementation of a fiber vibroscope [7], we used a tilted FBG to break the cylindrical symmetry of a non-PM multimode fiber and showed that launching linearly polarized light at orthogonal orientations relative to the tilt plane allowed for vectorial vibration information to be retrieved. Whenever working with cladding modes however, a suitable coupling mechanism must be provided to reintroduce the cladding mode light into the upstream core in order to allow remote interrogation with low loss. Any fiber discontinuity can be used for this purpose, as we have shown in [6–9]. In the new vectorial vibration sensing mechanism presented here, we avoid the uncertainties associated with the reproducibility and spectral quality of tilted gratings in multimode fiber by simply writing a conventional FBG in a short piece of PM-fiber spliced to standard single-mode fiber (Fig. 1). The key to the success of this device lies in the inherent small core mismatch between the two fibers, which allows the coupling of core and cladding modes. It will be shown below that the device thus constructed has far superior spectral qualities that facilitate sensor interrogation while being significantly simpler to fabricate. While the PM-FBG reflection spectrum contains the usual pair of resonances corresponding to the two orthogonal polarizations states of the core mode of the PM fiber, it also shows a group of additional resonances located about 6 nm away (on the short wavelength side) that are also polarization dependent and that react strongly to small fiber bending. We will show that these resonances correspond to modes coupled from the core of single-mode input fiber to a small subset of the cladding modes of the PM fiber. These modes propagate with little loss from the SMF to the PM fiber at the splice point, then get reflected by the FBG and partially recoupled back in the input SMF, to eventually return to the interrogation system. Most importantly, in contrast with earlier reports of ghost modes in tilted-FBG (a group of low-order cladding modes with overlapped spectra and complex polarizations [6,10]), the recoupled cladding modes in PM-FBG are well separated spectrally and show clear orthogonal polarization dependencies. As a result, both the orientation and the amplitude of the vibrations can be determined unambiguously via dual-path power detection of these recoupled orthogonal-polarimetric cladding modes. Meanwhile, the unwanted power fluctuations and temperature perturbations can be referenced out by monitoring the fundamental mode resonances (that remain unaffected by bending).

Figure 1 shows the schematic diagram of the vibration sensing system. We will show here that for X- or Y- polarized input light, the PM-FBG not only couples to different LP_{1n} cladding modes of the PM fiber but also that these cladding modes (and hence their spectral resonance in the reflection spectrum) have a very strong

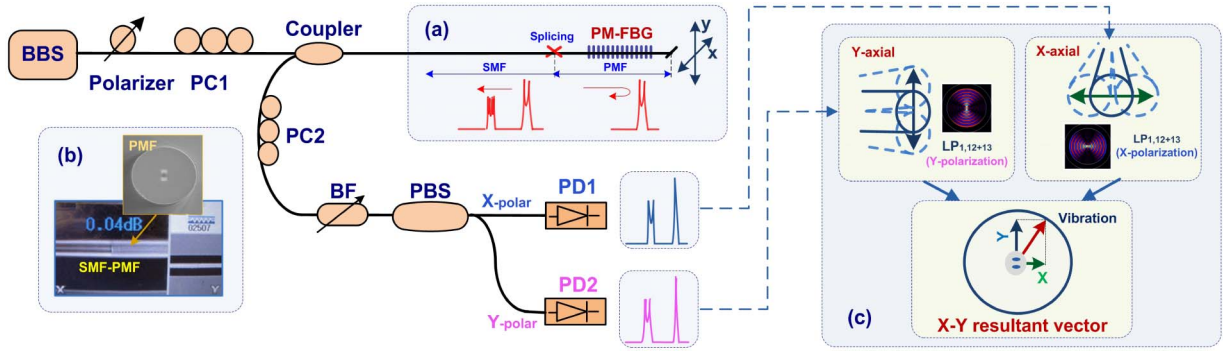

Fig. 1. (Color online) Schematic diagram of PM-FBG vector vibration sensing system. Inset (a) shows the configuration of the PM-FBG sensing probe, (b) shows the photograph of the SMF-PMF splicing point and the cross section of the "Bow Tie" PMF, and (c) presents the principle of X-Y profile vector analysis via orthogonal-polarimetric cladding-mode detections (X- and Y-polarization).

orientation dependence on bending that is associated with their polarization direction. The mode mismatch at the SMF-PMF junction to achieve this is minimal (the splicing loss at the junction is 0.04 dB). Once the reflected cladding modes are recoupled into the upstream SMF core, they are no longer affected by the vibration of the connecting fiber between the sensor and the interrogator. Figure 1(c) shows individual X- and Y-polarized LP_{1n} mode fields and their orientation relative to the stress members of the fiber (the vibration axis directions are also referenced to the same X and Y planes). These features amplitude of vibrations. The proposed sensing allows the construction of a very simple vector vibroscope that can determine the orientation, frequency, and configuration also provides temperature immunity, better reproducibility, and compact size (a single-ended device) for applications requiring embedding into structures.

As shown in Fig. 2, the reflection spectrum of the SMF-PMF (FBG) configuration shows four clear resonances with approximately equal spectral spacing on the short wavelength side of the dual reflection peaks corresponding to the core mode for the two polarizations. Here, an excellent alignment of the splicing between the SMF and PMF and short gap distance (several millimeters) between splicing point and gratings are necessary to maintain the polarization and symmetry of the modes across the junction. Meanwhile, the grating inscription should be moderate (not strong) to ensure each resonance present a well-defined profile.

In order to identify the additional modes appearing in the spectrum we used the Optigrating mode solver (from Optiwave) and found that these four resonances could be assigned to the $LP_{1,12}$ and $LP_{1,13}$ of the two polarizations. The following parameters for the PMF were used: "Bow-Tie" PM fiber with NA = 0.16 step index difference profile and diameters of 4.0/125 um. An FBG period of 0.5368 nm and length of 10 mm provided the best match to the experimental data. The mode field profiles associated with these resonances (shown in the insets of Fig. 3) clearly show that X- and Y-LP_{1n} modes do not possess cylindrical symmetry: it is this property that allows the vectorial sensitivity to bending that we now proceed to show.

Figure 1(a) shows the configuration of the sensing probe. An FBG (10 mm in length) is inscribed in a Fiber-core PMF using a pulsed KrF excimer laser and the phase-mask technique. A 15 mm long segment of the PMF containing the FBG was spliced to a 1 m long piece of SMF using a commercial Corning compact fusion splicer. The gap distance between the splice and the grating center was 7 mm. The fiber length downstream from the grating should be carefully selected as it works as the inertial mass, which dominates the sensor resonance

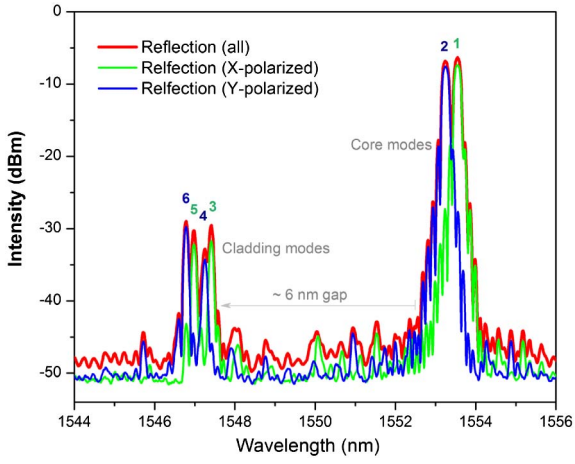

Fig. 2. (Color online) Reflection spectrum of PM-FBG under X- and Y-polarizations.

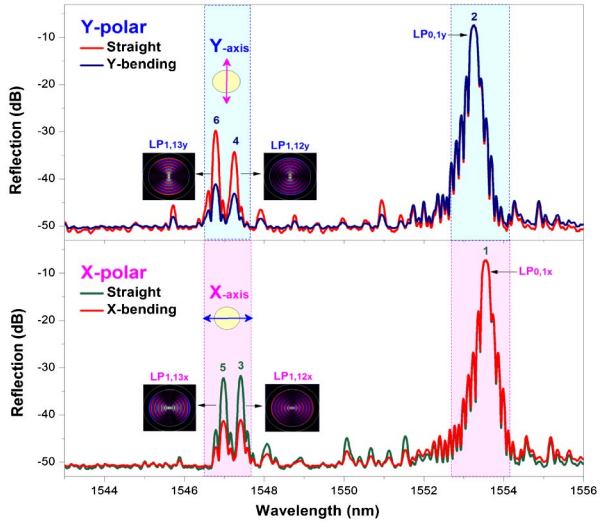

Fig. 3. (Color online) Comparison of two orthogonal polarimetric reflections (X- and Y-polarizations) of PM-FBG and their response to orthogonal-polarimetric bending (X- and Y-axis).

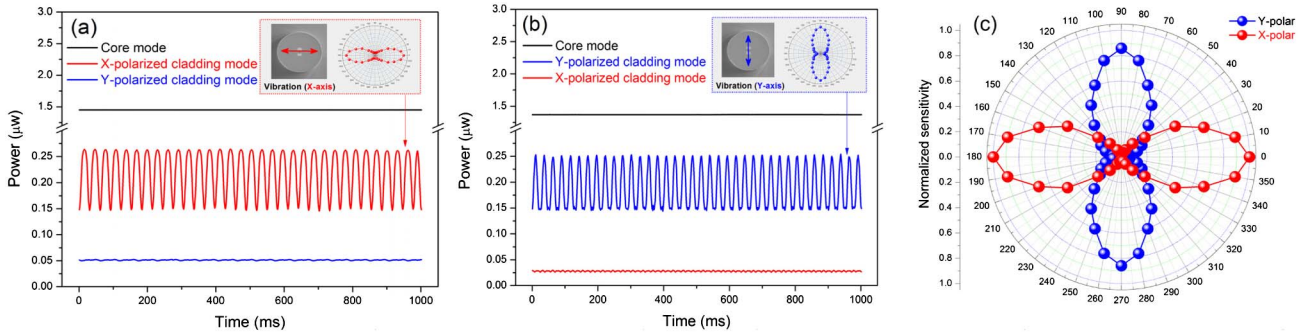

Fig. 4. (Color online) Real-time power output of PD1 (X-polarized $LP_{1,12+13}$ modes) and PD2 (Y-polarized $LP_{1,12+13}$ modes) under a given vibration (30 Hz) with different orientations of 0° (a), 90° (b) and the stable power references of the fundamental core mode (LP_{01}), where insets show the photographs of the cross section of PMF and their corresponding orthogonal-polarimetric sensitivity response; (c) angular dependence of vibration responsivity versus orthogonal-polarimetric orientation.

frequency and amplitude-frequency response [9]. Meanwhile, care must be taken to eliminate reflections from the end face of the PM fiber tip, since such reflections will return part of broadband light to the interrogation system and reduce the dynamic range of the measurement. The initial characterization of the sensor was carried out by launching light from an erbium amplified spontaneous emission broadband source into the sensing fiber through a 3 dB coupler, and measuring the reflected spectrum with a bandpass filter (BF) and a polarization beam splitter (PBS) followed by two power detectors (PDs) for vector analysis. Polarization control is essential for this system. Here, one polarizer and two polarization controllers (PCs) are used to line up the launch light (via PC1) and the PBS axes (via PC2) along the orthogonal orientations defined by the stress members of the PM-fiber, only then will the two PDs measure the "pure" polarized X and Y modes. Figure 3 shows the orthogonal-polarimetric PM-FBG reflections. The quality of the polarimetric orientation is validated by the spectral purity of the core mode reflections for the two orthogonal states (near 1554 nm). Simultaneously, it clearly appears that the four cladding modes near 1547 nm are really two pairs of X and Y modes. Upon bending of the fiber in the direction of the mode polarization, the coupling strength (at the splice and also at the FBG) decreases and the resonance power drops significantly.

What remains to be demonstrated is that the power reflected in each polarization state is independent of bending occurring in the orthogonal direction. Figure 4 demonstrates that the orientation of the applied vibrations can be recognized simply with dual-path power detection of the orthogonal-polarimetric X and Y modes. The fact that there are two modes for each polarization ($LP_{1,12}$ and $LP_{1,13}$) is not important here as the BFs are wide enough to cover both (and also any shifts arising from temperature fluctuations). Initial alignment of the system is performed simply by maximizing the power detected by PD1 when the fiber is kept straight and the input polarization rotated. The X-polarized spectrum is always found with the polarizer at 90° from the Y state. Meanwhile, Fig. 4 also shows that the LP_{01} modes are really insensitive to the fiber bending and can be used as references to remove any unwanted power fluctuations, regardless of the orientation of the vibrations. For vibration orientations over the full range from 0° to 360°, strong angular (oriented) dependence of the sensitivity response have been achieved along two orthogonal-polarimetric detections channels (X and Y axis) with minimal cross-sensitivity, as shown in Fig. 4(c).

A compact fiber-optic sensor for orientation recognized vibration measurement has been demonstrated. The interrogation of the sensor only requires two PCs, a PBS, two coarse BF, and two PDs. With filter passbands near 1 nm, the sensor response is immune to temperature fluctuations of several tens of degrees Celsius. The sensor (10 mm or less) does not require precise fabrication tolerances (in terms of Bragg wavelength, grating strength, or splicing alignment). An additional BF and PD combination can be used to monitor the bend-insensitive core mode reflection to cancel out power fluctuations.

This work was funded by the National Natural Science Foundation of China (61205080, 61235005), Guangdong Natural Science Foundation of China (S2011010001631, S2012010008385), Doctoral Program of Higher Education of China (20114401120006), Pearl River Scholar for Distinguished Young Scientist (2011J2200014). J. Albert is supported by the Natural Sciences and Engineering Research Council of Canada (NSERC) and the Canada Research Chairs Program.

References

1. F. Bosia, P. Giaccari, J. Botsis, M. Facchini, H. G. Limberger, and R. Salathé, Smart Mater. Struct. **12**, 925 (2003).
2. J. F. Botero-Cadavid, J. D. Causado-Buelvas, and P. Torres, IEEE J. Lightwave Technol. **28**, 1291 (2010).
3. M. S. Müller, H. J. El-Khozondar, T. C. Buck, and A. W. Koch, Opt. Lett. **34**, 2622 (2009).
4. R. Miao, W. Zhang, X. Feng, J. H. Zhao, and X. M. Liu, Appl. Opt. **48**, 709 (2009).
5. J. U. Thomas, N. Jovanovic, R. G. Krämer, G. D. Marshall, M. J. Withford, A. Tünnermann, S. Nolte, and M. J. Steel, Opt. Express **20**, 21434 (2012).
6. J. Albert, L. Y. Shao, and C. Caucheteur, Laser Photon. Rev. **7**, 83 (2013).
7. T. Guo, L. B. Shang, Y. Ran, B. O. Guan, and J. Albert, Opt. Lett. **37**, 2703 (2012).
8. T. Guo, A. Ivanov, C. K. Chen, and J. Albert, Opt. Lett. **33**, 1004 (2008).
9. T. Guo, L. Y. Shao, H. Y. Tam, P. Krug, and J. Albert, Opt. Express **17**, 20651 (2009).
10. B. Zhou, A. P. Zhang, B. B. Gu, and S. L. He, IEEE Photon. J. **2**, 152 (2010).